

Supplementary Information for

Boundaries and cross-link densities modulate domain sizes of polydomain nematic elastomers

Takuya Ohzono^{1*}, *Kaoru Katoh*², *Nariya Uchida*^{3*}

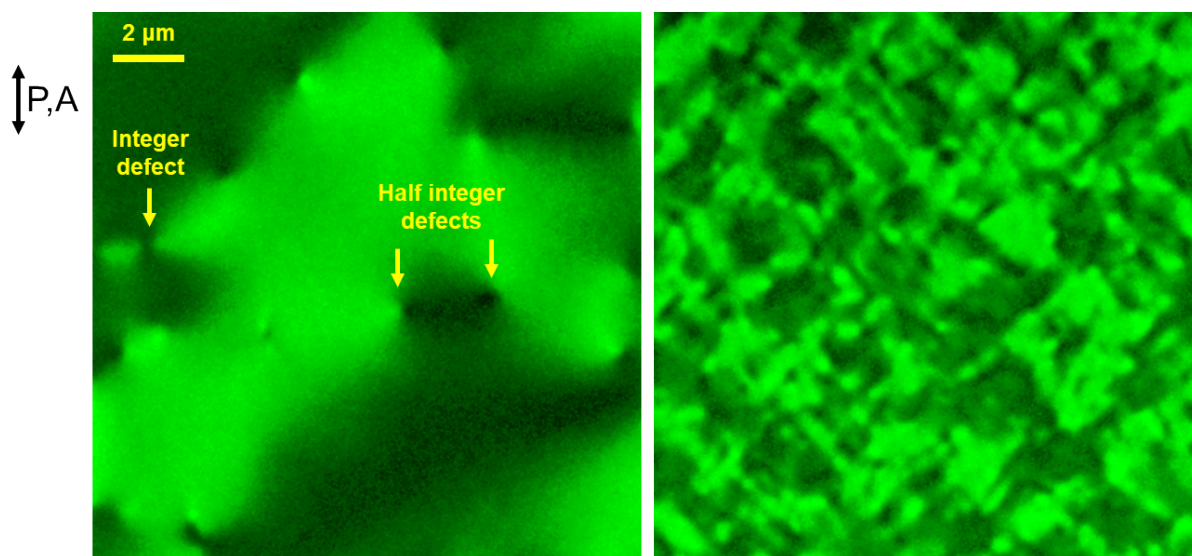
¹ Research Institute for Electronics and Photonics, National Institute of Advanced Industrial Science and Technology (AIST), 1-1-1 Higashi, Tsukuba 305-8565, Japan

² Biomedical Research Institute, AIST, 1-1-1 Higashi, Tsukuba 305-8566, Japan.

³ Department of Physics, Tohoku University, Sendai 980-8578, Japan.

E-mail: ohzono-takuya@aist.go.jp, uchida@cmpt.phys.tohoku.ac.jp

- **Fig. S1. cPFOM image of a low cross-link density sample.**
- **Fig. S2. A typical stress-strain curve of LCEs.**
- **Fig. S3. Point spread function (PSF) of the present cPFOM: Image of standard fluorescent beads in the present liquid crystal medium.**
- **Fig. S4. Determination of the interface from the 3D-cPFOM image slices with different focus position in the depth direction.**
- **Fig. S5. cPFOM images and ACF of X2.**
- **Fig. S6. cPFOM images and ACF of X3.**
- **Fig. S7. cPFOM images and ACF of X10.**



X1: Schlieren texture

X2: Polydomain texture

Fig. S1. cPFOM image of a low cross-link density sample. A sample (X1) containing half the amount of cross-linker of X2 becomes flowable, corresponding to the sol state without the self-supporting ability. The cPFOM image in left shows a typical schlieren texture with topological defects, pointed by arrows, as in the low molecular nematic LCs instead of the polydomain texture (right; X2)

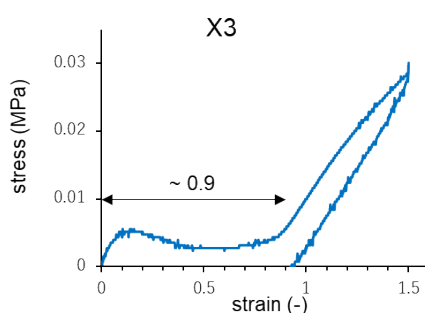


Fig. S2. A typical stress-strain curve of LCEs. Stress–strain curve of X3 at a strain rate of 0.0042 s^{-1} and at room temperature, showing the soft elasticity under strain of approximately 0.9. This value suggests that the elongation ratio upon the transition from the isotropic to nematic phase of our LCEs is in the order of 1.9 ($= 1 + 0.9$).

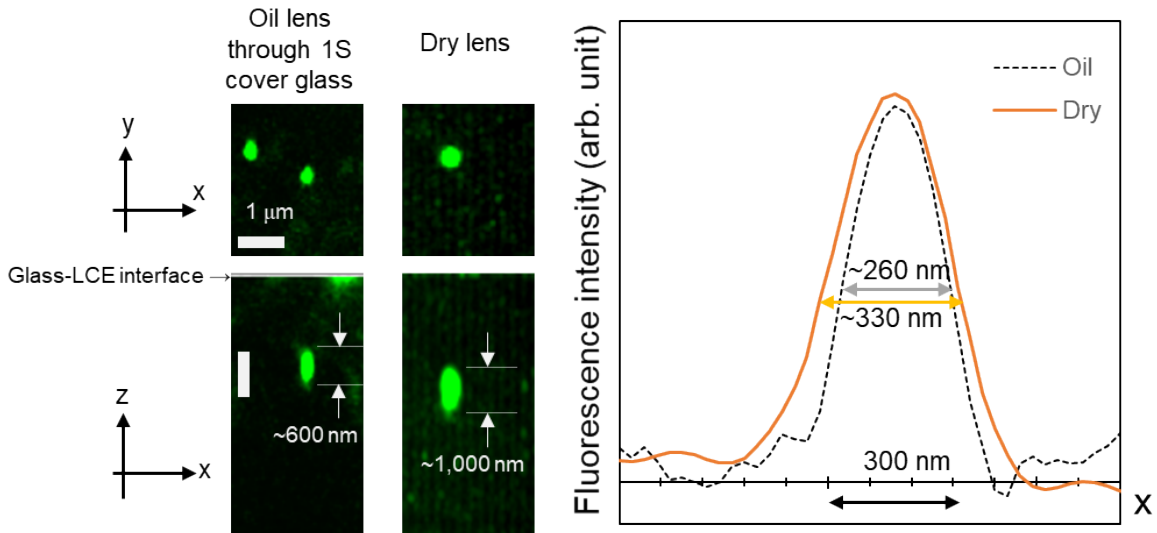


Fig. S3. Point spread function (PSF) of the present cPFOM: Image of standard fluorescent beads in the present liquid crystal medium. A LCE sample containing the green fluorescent standard beads with the diameter of 100 nm (FluoSpheres™ F8803, Thermofisher) instead of the C545T dye was observed with the cPFOM to gain the lens-dependent effect on the resolution. The images of the fluorescent beads show almost no blurring in the xy direction within the range of $\sim 3 \mu\text{m}$ from the glass interface. This supports that the present c-PFOM observation setup gives the true fluorescent intensity images within the range of $\sim 3 \mu\text{m}$ from the glass interface. The oil lens system ($NA \sim 1.45$) shows better resolutions in lateral (~ 260 nm: half maximum full width) and depth (~ 600 nm) directions than those of the dry one ($NA \sim 0.90$). In this study, the resolution for each lens setting is determined by the present actual measurements, thus allowing for a more accurate discussion of the lengths found in the experimental results than if one simply referred to the Rayleigh optical resolution, which can be calculated from NA and the light wavelength.

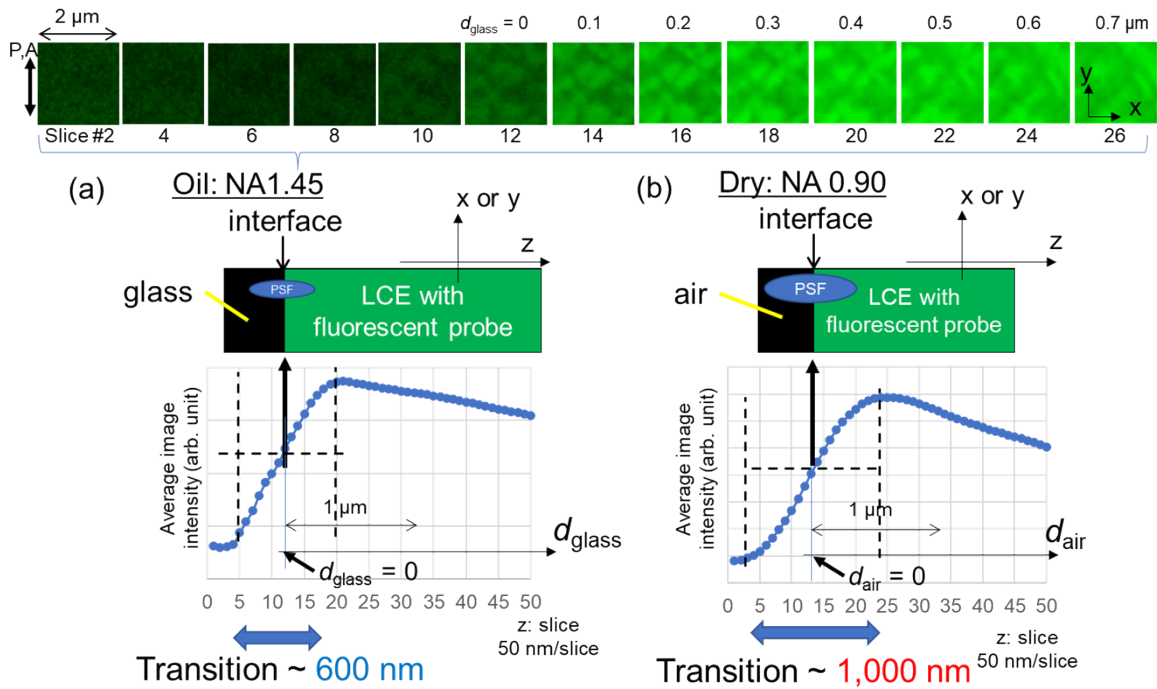


Fig. S4. Determination of the interface from the 3D-cPFOM image slices with different focus position in the depth direction. Although the sharp boundary is assumed, the average fluorescence intensity in the depth (z) direction should be blurred depending on the resolution in the direction. The lens-dependent point spread functions (PSF) shown in SI Fig. XX suggests that the degree of blurring is smaller for oil lens system due to the smaller PSF in the depth direction. As an example, a set of image stacks in the z direction from the glass side to the LCE through the interface is shown in the top. The corresponding average fluorescence intensities regarding the slice number is plotted in (a). As expected, the interface appeared with a transition range, which roughly corresponded to the PSF in the z direction. As the focal point went into the sample, the intensity monotonically increased, and it reached the maximum, at which almost the whole PSF is in the LCE. Then, the intensity gradually decreased because the excitation light intensity was reduced by the absorption by the fluorescent probes outside the focus. As a result, the middle point of the first intensity increase, indicated by the bold arrow guided by dashed lines, may be regarded as the correct interface, at which the focal point was positioned at the interface. Indeed, the clear polydomain texture started appearing around this slice. This point was defined as the interface, where the depth from the interface $d_x = 0$ ($x =$

glass or air depending on the media in contact). In the case of the dry lens, the interface transition range became larger because of the larger PSF as shown in (b).

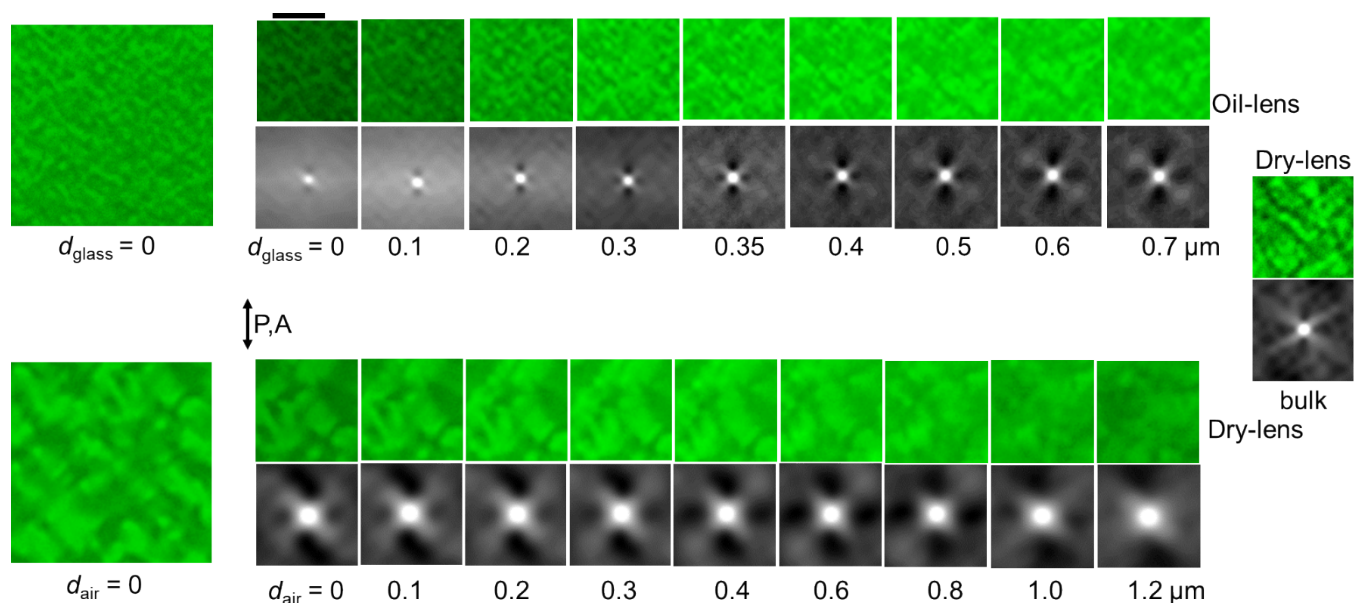


Fig. S5. cPFOM images and ACF of X2. Each slice image and ACF with the representative wide-area images.

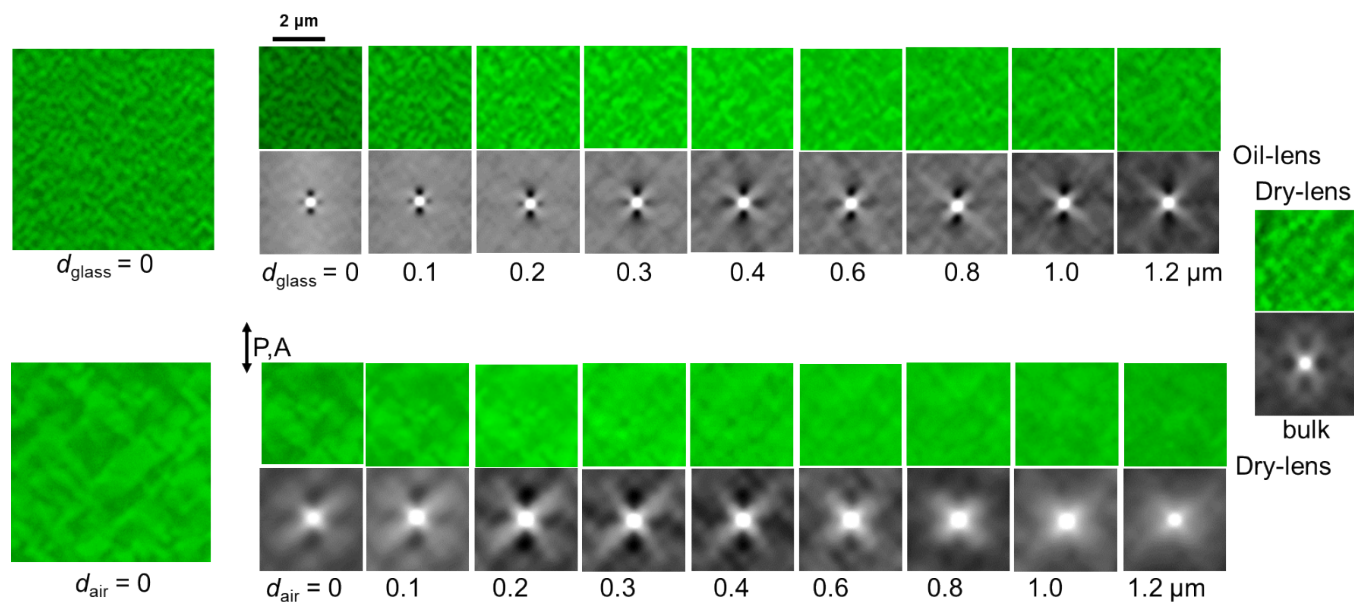


Fig. S6. cPFOM images and ACF of X3. Each slice image and ACF with the representative wide-area images.

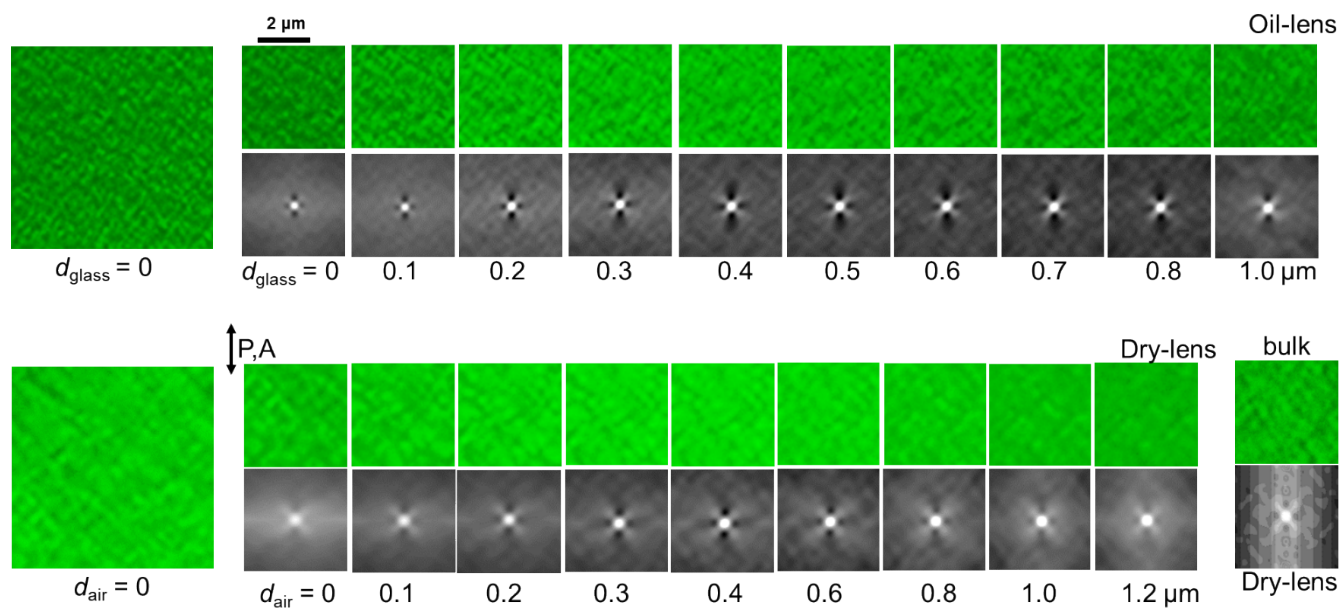


Fig. S7. cPFOM images and ACF of X10. Each slice image and ACF with the representative wide-area images.